# Journal of Materials Chemistry A



### COMMUNICATION

View Article Online
View Journal | View Issue



Cite this: J. Mater. Chem. A, 2019, 7, 19691

Received 3rd June 2019 Accepted 9th August 2019

DOI: 10.1039/c9ta05885k

rsc.li/materials-a

# Chemically inert covalently networked triazolebased solid polymer electrolytes for stable allsolid-state lithium batteries†

Yi Shi, \$\bigcup\_{\mathbb{c}}\$\footnote{\mathbb{c}}\$ Yang Chen, \$\dot{\mathbb{c}}\$ a Yanliang Liang, \$\bigcup\_{\mathbb{c}}\$\dot{\mathbb{c}}\$ and Yan, \$\dot{\mathbb{c}}\$ And Panerjee, \$\bigcup\_{\mathbb{c}}\$ And Panerjee, \$\bigcup\_{\mathbb{c}}\$ Haleh Ardebili, \$\dot{\mathbb{d}}\$ Megan L. Robertson, \$\bigcup\_{\mathbb{c}}\$ axiaoli Cui \$\bigcup\_{\mathbb{c}}\$ and Yan Yao \$\bigcup\_{\mathbb{c}}\$\*a

Covalently networked polymers offer desirable non-crystallinity and mechanical strength for solid polymer electrolytes (SPEs), but the chemically active cross-links involved in their construction could deteriorate the compatibility with high-energy cathode materials that are electrophilic and/or in the charged state. Herein we reveal a strong dependence of cyclability of such cathodes on the reactivity of covalently networked SPEs and demonstrate a polymer design that renders these SPEs chemically inert. We designed and synthesized two hybrid networks, both with polyethylene oxide as the cation conducting component and polyhedral oligomeric silsesquioxane as the branch point, but respectively use alkylamino and chemically inert triazole groups as cross-links. All-solid-state cells using the alkylamino-containing SPE underwent rapid degradation while cells using triazole SPEs showed stable cycling.

High-energy and safe lithium batteries for electrical energy storage and power supply have attracted tremendous interest because lithium metal has the highest theoretical capacity (3860 mA h g<sup>-1</sup>) and lowest electrochemical potential (-3.04 V) among metal anodes.<sup>1,2</sup> However, metallic lithium dendrite growth and flammable liquid electrolytes and their side reactions with lithium metal compromise the safety of lithium batteries. Solid electrolytes may physically block lithium dendrites and avoid the flammability issues of liquid electrolytes, thereby leading to safe lithium batteries.<sup>3-9</sup> Various solid electrolytes have been reported to date, <sup>10-16</sup> among which solid polymer electrolytes (SPEs) based on polyethylene oxide (PEO) have received considerable attention owing to their strong lithium-ion solvating ability, easy processing, low density, and tunable structure.<sup>17,18</sup> SPEs based on unmodified PEO show low

ionic conductivity and mechanical strength which have limited their application as solid electrolytes. Several strategies have been developed to solve these problems, such as using PEObased block/star/graft copolymers, 19-24 nanostructured polymers,25-28 composite polymers,29,30 networked polymers,3,8,31,32 etc. In particular, covalently networked SPEs showed high ionic conductivity, great mechanical strength and excellent lithium dendrite growth resistance. 3,4,8 However, most cross-linked SPEs were prepared via polymerization aided by radical initiators or catalysts such as free radicals, which are highly reactive with lithium metal.24,33-35 Recently, catalyst-free organic curing reactions such as the epoxy-amino curing (EAC) reaction have been used to prepare cross-linked SPEs. 4,8,36 However, the formed alkylamino groups are known to have low anodic stability.37,38 While these SPEs appeared to be stable when paired with LiFeO<sub>4</sub> which is non-electrophilic when assembled into a cell and requires a relatively low charging potential among commercial lithium cathode materials, we found that, as will be shown below, they have compatibility issues with several other categories of cathode materials, with which high-energy lithium batteries are being researched. It remains a challenge to develop SPEs that simultaneously provide high ionic conductivity, mechanical strength, and chemical inertness toward both lithium metal and high-voltage cathode materials.

Herein, we used a catalyst-free azide-alkyne cycloaddition (AAC) reaction to prepare a chemically inert and covalently networked hybrid polymer electrolyte, PEO-ta-POSS (Fig. 1a), where PEO serves as the lithium-ion solvating component, the inorganic polyhedral oligomeric silsesquioxane (POSS) as the branch point, and, most importantly, oxidation-resistant triazole (ta) as the cross-link. For comparison, PEO-amine-POSS

<sup>&</sup>lt;sup>a</sup>Department of Electrical and Computer Engineering, TcSUH, University of Houston, Houston, Texas 77204, USA. E-mail: yyao4@uh.edu

<sup>&</sup>lt;sup>b</sup>Department of Materials Science, Fudan University, Shanghai 200433, China

Department of Materials Science and Engineering, Texas A&M University, Texas

<sup>&</sup>lt;sup>4</sup>Department of Mechanical Engineering, University of Houston, Houston, Texas 77204. USA

<sup>&</sup>lt;sup>e</sup>Department of Chemical and Biomolecular Engineering, University of Houston, Houston, Texas 77204, USA

 $<sup>\</sup>dagger$  Electronic supplementary information (ESI) available. See DOI: 10.1039/c9ta05885k

<sup>‡</sup> These authors contributed equally.

<sup>§</sup> Current address: School of Materials Science and Engineering, Sun Yat-Sen University, Guangzhou 510275, China.

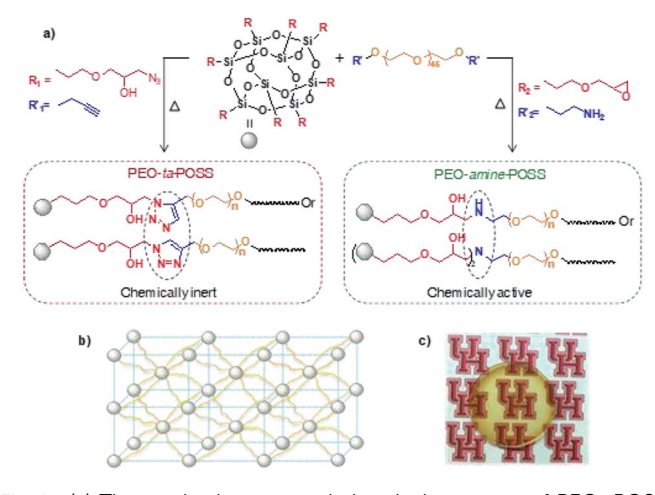


Fig. 1 (a) The synthesis route and chemical structure of PEO-POSS cross-linked SPEs, (b) schematic structure of the network, and (c) photograph of a 200  $\mu$ m-thick membrane of 4PEO-ta-POSS.

with alkylamino groups as the cross-link was also prepared. A series of cathode materials with varying properties were used to investigate the electrochemical performance of the SPEs, including poly(benzoquinonyl sulfide) (PBQS),  $^{39}$  a representative of organic carbonyl compounds which are electrophilic and expected to be high-energy cathodes for lithium batteries;  $^{40,41}$   $\xi$ -V<sub>2</sub>O<sub>5</sub>, a high-capacity intercalation compound that has a high open-circuit voltage of 3.8 V  $\nu$ s. Li $^+$ /Li and could deliver higher energy than most commercial cathodes;  $^{42}$  and LiFePO $_4$ ,  $^{43}$  by far the most investigated cathode in SPE studies. We show that the chemical inertness of PEO-ta-POSS is critical for achieving high capacity and stable cycling.

Hybrid SPEs are easily constructed via a catalyst-free organic curing reaction between functionalized POSS and PEO in the presence of LiTFSI ([EO]: [Li] = 16:1) in a one-pot process. The functionalized POSS and PEO as well as LiTFSI were dissolved in acetonitrile, and then the solution was drop-cast in a PTFE mold. A thin membrane of cross-linked PEO-POSS SPEs was obtained after curing and thorough removal of solvent (Fig. 1c). The nPEO-ta-POSSs (n = 2, 4, and 6, n denotes the molar ratio of 1PEO to POSS) were synthesized from POSS-(N<sub>3</sub>)<sub>8</sub> (Fig. 1 and S1 in the ESI†) and PEO-dialkynyl (Fig. 1 and S2†). As shown in Fig. S3a and b,† the characteristic absorption of azido groups at 2111 cm<sup>-1</sup> was absent when the molar ratio of [PEO]: [POSS] was 4:1 and 6:1, and the characteristic absorption of alkynyl groups at 2740 cm<sup>-1</sup> disappeared when the molar ratio of [PEO]: [POSS] was 2:1 and 4:1, indicating a complete AAC coupling reaction and formation of a cross-linked network. The azido and alkynyl absorption bands remained when the molar ratio of [PEO]: [POSS] was 2:1 and 6:1 due to an excess of POSS-(N<sub>3</sub>)<sub>8</sub> and PEO-dialkynyl, respectively. Meanwhile, 4PEOamine-POSS was prepared by the EAC reaction and confirmed by FT-IR: after the reaction, the absorption of epoxy groups at 907 cm<sup>-1</sup> disappeared, indicating a complete reaction between epoxy and alkylamino groups and formation of a cross-linked network (Fig. S4†).

The phase behaviors of the hybrid SPEs were studied by differential scanning calorimetry (DSC). All the hybrid SPEs only show the glass transition and no melting points, indicating that the crystallization of PEO is completely suppressed (Fig. 2a). The amorphous phases were confirmed using the peak-less XRD patterns (Fig. 2b). The mechanical properties of the cross-linked SPEs were measured by dynamic mechanical analysis (DMA) in tensile mode (Fig. 2c and Table 1). All SPEs except 6PEO-ta-POSS show constant storage moduli (E') above the glass transition temperature and up to 130 °C. 6PEO-ta-POSS shows increased E' between 0 and 40 °C due to cold crystallization.3 Such thermal stability contrasts with that of PEO-based electrolytes which soften/melt at >60 °C. The modulus of PEO-ta-POSS reaches a maximum at a [PEO]: [POSS] ratio of 4: 1 when the azido and alkynyl groups are in equimolar amounts. Fig. 2d shows the temperature-dependent ionic conductivity of cross-linked SPEs. At room temperature, the conductivity of PEO-ta-POSS SPEs is one to two orders of magnitude higher than that of PEO  $(\sim 10^{-6} \text{ S cm}^{-1})$  and comparable to the best reported values  $(\sim 10^{-4} \text{ S cm}^{-1})$  for crosslinked SPEs.<sup>3,44-46</sup> The ionic conductivity of PEO-ta-POSS SPEs increases from 1.5  $\times$  10<sup>-4</sup> (2PEO-ta-POSS) to  $5.9 \times 10^{-4}$  (4PEO-ta-POSS) to  $1.2 \times 10^{-3}$  S cm<sup>-1</sup> (6PEOta-POSS) at 90 °C, which is attributed to the increasing PEO content. The ionic conductivity of 4PEO-amine-POSS 3.8 ×  $10^{-4}$  S cm<sup>-1</sup> is close to that of 4PEO-ta-POSS. In this study, ionic conduction mainly depends on the PEO segments, and the triazole groups mainly serve as the cross-link. Other stable functional groups may also serve as the cross-link, provided that they can be formed via reactions that have near-unity yields under mild conditions. The ionic conductivities are further fitted using the Vogel-Tammann-Fulcher (VTF) model (Fig. S5†),46 and the ionic transport activation energy is 8.4 kJ  $\text{mol}^{-1}$  (2PEO-ta-POSS), 8.2 kJ  $\text{mol}^{-1}$  (4PEO-ta-POSS), 7.8 kJ  $\text{mol}^{-1}$  (6PEO-ta-POSS), and 8.3 kJ  $\text{mol}^{-1}$  (4PEO-amine-POSS) (Table S1†). This result agrees with a previous analysis in which, within the same electrolyte class, a high ionic conductivity corresponds to a small activation energy. 44,46

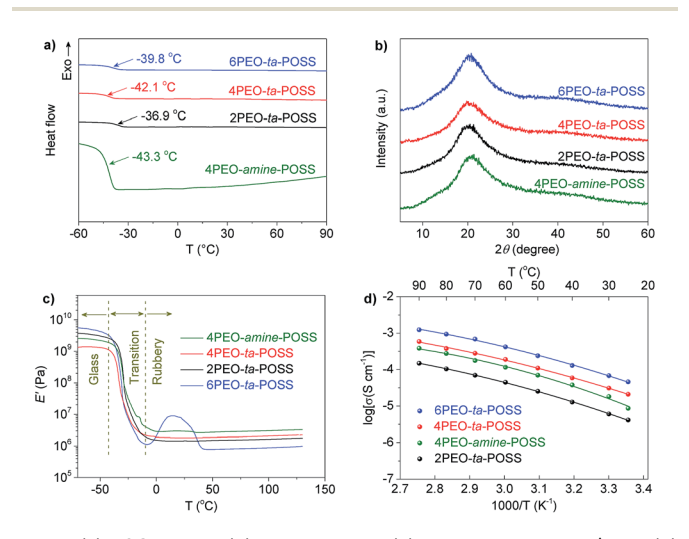


Fig. 2 (a) DSC curves, (b) XRD patterns, (c) storage modulus E', and (d) ionic conductivity of PEO-POSS cross-linked polymer electrolytes.

Sample <sup>a</sup>	Molar ratio (PEO : POSS)	PEO content (wt%)	$T_{ m g}  (^{\circ}{ m C})$	E' (MPa)	$\sigma$ (S cm <sup>-1</sup> )			
					30 °C	60 °C	90 °C	$t\left(\mathrm{Li}^{\scriptscriptstyle{+}}\right)$
2PEO-ta-POSS	2:1	71.6	-36.9	1.6	$6.1\times10^{-6}$	$4.5\times10^{-5}$	$1.5 imes10^{-4}$	0.17
4PEO-ta-POSS	4:1	83.5	-42.1	2.0	$3.1 \times 10^{-5}$	$1.9\times10^{-4}$	$5.9\times10^{-4}$	0.30
6PEO-ta-POSS	6:1	88.4	-39.8	0.9	$6.8 \times 10^{-5}$	$4.2\times10^{-4}$	$1.2\times10^{-3}$	0.20
4PEO-amine-POSS	4:1	85.9	-43.3	3.0	$1.8\times10^{-5}$	$1.1\times10^{-4}$	$3.8\times10^{-4}$	0.11

<sup>&</sup>lt;sup>a</sup> All samples had LiTFSI, [EO]:  $[Li^+] = 16:1$ .

Li/PEO-POSS SPE/Li symmetric cells were assembled to evaluate Li/SPE interfacial stability. Galvanostatic lithium plating and stripping performance was recorded at 0.3 mA cm<sup>-2</sup> with a specific capacity of 0.3 mA h cm<sup>-2</sup> (Fig. S6†). Compared to 2PEO-ta-POSS, 4PEO-ta-POSS and 6PEO-ta-POSS showed better stability and lower voltage polarization with initial area specific resistances (ASRs) of 312 and 318  $\Omega$  cm<sup>2</sup>, respectively, which benefited from the higher ionic conductivities. The voltage profiles agree with the Li<sup>+</sup> transference number: a higher Li<sup>+</sup> transference number (Tables 1 and S2, Fig. S7†) corresponds to a flatter voltage plateau. 47,48 In 4PEO-amine-POSS, the amino group can coordinate with Li-ions and trap them as defect sites; this interaction may have led to the lower Li-ion transference number. The Li-ion transference number of 4PEO-ta-POSS is the largest among the xPEO-ta-POSSs because it comprises the least unreacted functional groups (e.g. alkynyl and azido groups) which may coordinate with Li-ions. Even higher transference number may be possible if less coordinating polymers such as cyano-containing ones are used in place of PEO.

The electrochemical stability of PEO-ta-POSS and PEOamine-POSS SPEs was evaluated using Li/PEO-POSS SPE/C cells where the cathode is composed of a mixture of the SPEs and conductive carbon (Fig. 3a). Such a composite electrode is

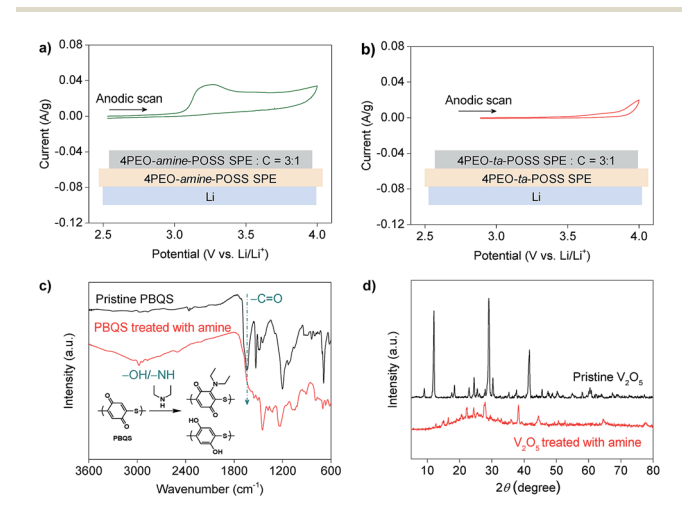


Fig. 3 The electrochemical and chemical stability of PEO-POSS SPEs. CV curves of (a) Li/PEO-amine-POSS SPE/C and (b) Li/PEO-ta-POSS SPE/C cells at  $0.2 \text{ mV s}^{-1}$ . (c) The FT-IR spectra of PBQS before and after treatment with amines. (d) The XRD patterns of V<sub>2</sub>O<sub>5</sub> before and after treatment with amines.

a close approximation of a battery cathode where the SPE and conductive carbon are thoroughly mixed and have a large contact area. The electrode can therefore more precisely measure the electrochemical stability window of SPEs than a traditional planar electrode which has a limited contact area.49,50 A broad irreversible anodic peak appears above 3.0 V for 4PEO-amine-POSS, indicating instability of the polymer at high potentials. In contrast, anodic current was only observed above 3.8 V for 4PEO-ta-POSS. The chemical stability of the SPEs was probed by directly treating cathode materials with diethylamine, which resembles the dialkylamino group in 4PEOamine-POSS. A suspension of PBQS in a solution of diethylamine in tetrahydrofuran was stirred at room temperature for 12 h. The C=O absorption of PBQS at 1647 cm<sup>-1</sup> almost disappeared after the reaction, and a broad absorption at 3129 cm<sup>-1</sup> corresponding to -OH appeared, indicating that the majority of quinone units had been converted into hydroquinone (Fig. 3b). A similar model reaction between V2O5 and diethylamine led to a complete conversion of V2O5 into an unidentified compound, as detected in the XRD patterns (Fig. 3c). These undesired reactions become more severe at the cell testing temperatures (60-90 °C).

The cell performances of PEO-ta-POSS and PEO-amine-POSS SPEs were investigated in lithium cells at 90 °C. The Li/4PEO-ta-POSS SPE/PBQS cell showed a stable capacity of 153 mA h  $g^{-1}$  at 0.1C (Fig. 4a), while the capacity of Li/4PEO-amine-POSS SPE/ PBQS decreased from 62 to 50 mA h  $g^{-1}$  in the first 3 cycles with large irreversible charge capacities (Fig. 4b). After 50 cycles, the stable capacity of Li/4PEO-amine-POSS SPE/PBOS was only 35 mA h g<sup>-1</sup>, a quarter of that of Li/4PEO-ta-POSS SPE/PBQS (Fig. 4c). A similar stability difference was found for Li/PEO-POSS SPE/V<sub>2</sub>O<sub>5</sub> cells. The Li/4PEO-ta-POSS SPE/V<sub>2</sub>O<sub>5</sub> cell showed a reversible specific capacity of 245 mA h g<sup>-1</sup> and maintained 223 mA h g<sup>-1</sup> after 50 cycles, corresponding to a 91% capacity retention (Fig. 4d and f). The Li/4PEO-amine-POSS SPE/V2O5 cell showed a low coulombic efficiency in the first cycle and lost 95% of its initial capacity after 10 cycles (Fig. 4e and f). The inferiority of the SPEs with the alkylamino cross-link was not reported in the literature probably because of the cathode material used in previous covalently networked SPE studies, which was almost always LiFePO4. The performance difference between the two SPEs was not as drastic as that with a LiFePO<sub>4</sub> cathode: while the Li/4PEO-ta-POSS SPE/LiFePO<sub>4</sub> cell showed a higher and more stable specific capacity of 156 mA h g $^{-1}$  (Fig. S8a $^{\dagger}$ ), the Li/4PEO-amine-POSS SPE/LiFePO $_4$ 

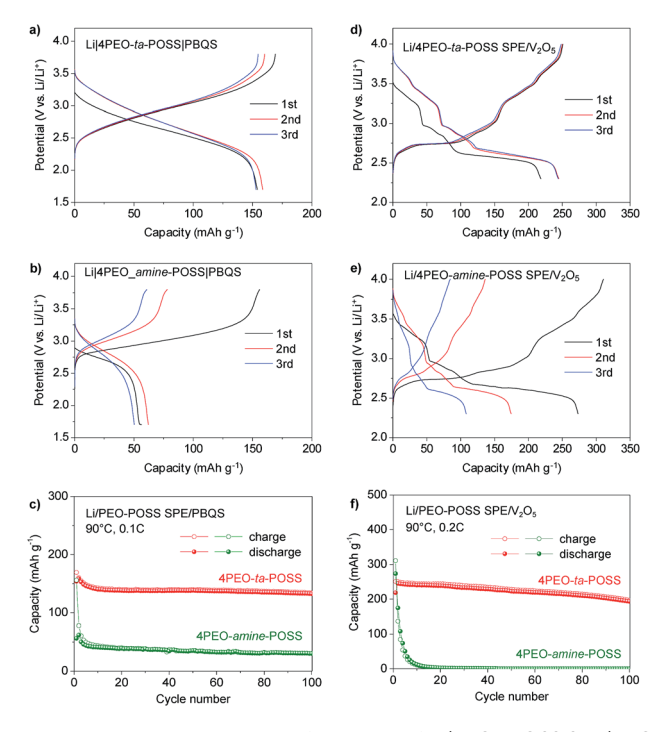


Fig. 4 The electrochemical performance of Li/PEO-POSS SPE/PBQS (a–c) and Li/PEO-POSS SPE/ $V_2O_5$  cells (d–f) at 90 °C. (a and d) The voltage profiles of the first three cycles using 4PEO-ta-POSS SPE. (b and e) The voltage profiles of the first three cycles using 4PEO-ta-POSS SPE. (c and f) Comparison of the cycling performance of each cathode material in the two SPEs.

cell held on its own a usable though less stable specific capacity of  $\sim$ 120 mA h g<sup>-1</sup> (Fig. S8b†).

We have checked the morphology of Li/SPE/PBQS cells after 300 cycles. Fig. S9† shows the cross-sectional SEM images of the cells using (a and c) 4PEO-amino-POSS SPE and (b and d) 4PEO-ta-POSS SPE, respectively. In Fig. S9(a),† interdiffusion between cathode materials and 4PEO-amino-POSS polymer electrolytes was observed as the result of the chemical reaction between PBQS and the 4PEO-amino-POSS SPE, leading to the absence of a cathode-SPE interface. In contrast, a clear cathode-SPE interface between PBQS and the proposed 4PEO-ta-POSS SPE can be observed in Fig. S9(b),† indicating the chemical inertness. A uniform lithium deposition, as seen in Fig. S9(c and d),† indicates that both 4PEO-amino-POSS and 4PEO-ta-POSS SPEs can suppress the growth of lithium dendrites. Note that some lithium was plated on the surface of the 4PEO-ta-POSS SPE at the interface, which may result in an increase of Li-SPE interfacial resistance.

The AC impedance of Li/4PEO-amino-POSS SPE/PBQS and Li/4PEO-ta-POSS SPE/PBQS cells after 300 cycles was also measured over a frequency range of  $10^6$  to 0.1 Hz with a 7 mV amplitude. The plots were fitted with the inserted equivalent circuit models using ZView software, and the corresponding parameters are listed in Tables S3 and S4.†  $R_{\rm e}$  stands for bulk resistance of the polymer electrolyte;  $R_{\rm 1}$  and CPE<sub>1</sub> represent the charge transfer resistance and interfacial capacitance of the Li–SPE interface;  $R_{\rm 2}$  and CPE<sub>2</sub> represent the charge transfer resistance and interfacial capacitance of the cathode–SPE interface;

W stands for the Warburg resistance. Fig. S10(c and d)† show the Nyquist plots of cycled Li/4PEO-amino-POSS SPE/PBQS and Li/4PEO-ta-POSS SPE/PBQS cells. Upon cycling, the polymers and LiTFSI decompose continuously on the lithium surface, <sup>36,51</sup> leading to an enlargement of  $R_{\rm e}$  and  $R_{\rm 1}$  compared with those of the fresh cells. The cathode–SPE interfacial resistance ( $R_{\rm 2}$ ) of the Li/4PEO-ta-POSS SPE/PBQS cell was about one eighth that of the Li/4PEO-ta-POSS SPE/PBQS cell. The chemical reaction between PBQS and the 4PEO-ta-POSS SPE leads to a well-contacted cathode–SPE interface, and thus a much smaller interfacial resistance.

The examples above show that the (electro)chemical inertness of SPEs is a prerequisite for using high-energy cathode materials in a covalently networked SPE-based solid-state cell. The use of triazole as an unreactive crosslink for PEO-POSS eliminates the anodic instability and chemical reactivity found for alkylamino and alkyl sulfide groups typically used for constructing such polymers. The fact that all three cathode materials work satisfactorily in the electrolyte indicates the universality of the strategy for high-performance SPE design.

#### Conclusions

In summary, we have developed covalently networked polymer electrolytes cross-linked by triazole groups via a facile catalystfree AAC reaction for all-solid-state lithium batteries. The polymer design avoids residual reactive agents and cross-link groups in the electrolyte, thus leading to (electro)chemical inertness rarely found in covalently networked SPEs. The triazole-based PEO-ta-POSS SPEs expand the electrochemical stability window by 800 mV compared with a structurally similar SPE cross-linked by alkylamino groups. Multiple categories of potentially high-energy cathode materials were found to charge and discharge stably in the PEO-ta-POSS SPEs, whereas they all undergo rapid capacity fading in the alkylamino-based SPE. Control cells and reactions indicate a strong dependence of cell performance on the reactivity of the SPEs. Our approach provides a new design space for developing polymer electrolytes that simultaneously offer mechanical strength, ionic conductivity, and, most importantly, chemical stability for SPE-based solid state batteries.

#### Conflicts of interest

There are no conflicts to declare.

## Acknowledgements

We acknowledge the funding support from the U.S. Department of Energy's Office of Energy Efficiency and Renewable Energy (EERE), as part of the Battery 500 Consortium (# DE-EE0008234). Y. C. acknowledges funding from China Scholarship Council. J. A. and S. B. acknowledge support from the National Science Foundation under DMR 1809866. M. L. R and W. D. acknowledge support from the National Science Foundation under DMR 1351788.

#### Notes and references

Communication

- 1 W. Xu, J. Wang, F. Ding, X. Chen, E. Nasybulin, Y. Zhang and J.-G. Zhang, *Energy Environ. Sci.*, 2014, 7, 513–537.
- 2 Y. Lu, Z. Tu and L. A. Archer, Nat. Mater., 2014, 13, 961.
- 3 R. Khurana, J. L. Schaefer, L. A. Archer and G. W. Coates, J. Am. Chem. Soc., 2014, 136, 7395–7402.
- 4 Q. Lu, Y. B. He, Q. Yu, B. Li, Y. V. Kaneti, Y. Yao, F. Kang and Q. H. Yang, *Adv. Mater.*, 2017, 29, 1604460.
- 5 X.-X. Zeng, Y.-X. Yin, N.-W. Li, W.-C. Du, Y.-G. Guo and L.-J. Wan, *J. Am. Chem. Soc.*, 2016, **138**, 15825–15828.
- 6 A. Sharafi, E. Kazyak, A. L. Davis, S. Yu, T. Thompson, D. J. Siegel, N. P. Dasgupta and J. Sakamoto, *Chem. Mater.*, 2017, 29, 7961–7968.
- 7 F. Han, J. Yue, X. Zhu and C. Wang, *Adv. Energy Mater.*, 2018, **8**, 1703644.
- 8 Q. Pan, D. M. Smith, H. Qi, S. Wang and C. Y. Li, *Adv. Mater.*, 2015, 27, 5995–6001.
- P. Zhu, C. Yan, J. Zhu, J. Zang, Y. Li, H. Jia, X. Dong, Z. Du,
   C. Zhang, N. Wu, M. Dirican and X. Zhang, *Energy Storage Materials*, 2019, 17, 220–225.
- 10 A. Varzi, R. Raccichini, S. Passerini and B. Scrosati, J. Mater. Chem. A, 2016, 4, 17251–17259.
- 11 H. Zhang, C. Li, M. Piszcz, E. Coya, T. Rojo, L. M. Rodriguez-Martinez, M. Armand and Z. Zhou, *Chem. Soc. Rev.*, 2017, 46, 797–815.
- 12 Z. Zhu, M. Hong, D. Guo, J. Shi, Z. Tao and J. Chen, *J. Am. Chem. Soc.*, 2014, **136**, 16461–16464.
- 13 J. Janek and W. G. Zeier, Nat. Energy, 2016, 1, 16141.
- 14 J. Zhang, X. Li, Y. Li, H. Wang, C. Ma, Y. Wang, S. Hu and W. Wei, *Front. Chem.*, 2018, **6**, 168.
- 15 Q. Wang, H. Zhang, Z. Cui, Q. Zhou, X. Shangguan, S. Tian, X. Zhou and G. Cui, *Energy Storage Materials*, 2019, DOI: 10.1016/j.ensm.2019.04.016.
- 16 J. Zhang, J. Zhao, L. Yue, Q. Wang, J. Chai, Z. Liu, X. Zhou, H. Li, Y. Guo, G. Cui and L. Chen, *Adv. Energy Mater.*, 2015, 5, 1501082.
- 17 M. A. Morris, H. An, J. L. Lutkenhaus and T. H. Epps, *ACS Energy Lett.*, 2017, 2, 1919–1936.
- 18 Z. Xue, D. He and X. Xie, *J. Mater. Chem. A*, 2015, 3, 19218–19253.
- 19 P. R. Chinnam and S. L. Wunder, *Chem. Mater.*, 2011, 23, 5111–5121.
- 20 Y. Chen, Y. Shi, Y. Liang, H. Dong, F. Hao, A. Wang, Y. Zhu, X. Cui and Y. Yao, ACS Appl. Energy Mater., 2019, 2, 1608–1615.
- 21 C. M. Bates, A. B. Chang, N. Momčilović, S. C. Jones and R. H. Grubbs, *Macromolecules*, 2015, **48**, 4967–4973.
- 22 R. Bouchet, S. Maria, R. Meziane, A. Aboulaich, L. Lienafa, J.-P. Bonnet, T. N. T. Phan, D. Bertin, D. Gigmes, D. Devaux, R. Denoyel and M. Armand, *Nat. Mater.*, 2013, 12, 452.
- 23 R. Bouchet, T. N. T. Phan, E. Beaudoin, D. Devaux, P. Davidson, D. Bertin and R. Denoyel, *Macromolecules*, 2014, 47, 2659–2665.
- 24 J. Ping, H. Pan, P. P. Hou, M.-Y. Zhang, X. Wang, C. Wang, J. Chen, D. Wu, Z. Shen and X.-H. Fan, ACS Appl. Mater. Interfaces, 2017, 9, 6130–6137.

- 25 G. Yang, C. Chanthad, H. Oh, I. A. Ayhan and Q. Wang, J. Mater. Chem. A, 2017, 5, 18012–18019.
- 26 M. W. Schulze, L. D. McIntosh, M. A. Hillmyer and T. P. Lodge, *Nano Lett.*, 2014, **14**, 122–126.
- 27 L. D. McIntosh, M. W. Schulze, M. T. Irwin, M. A. Hillmyer and T. P. Lodge, *Macromolecules*, 2015, 48, 1418–1428.
- 28 E. Glynos, L. Papoutsakis, W. Pan, E. P. Giannelis, A. D. Nega, E. Mygiakis, G. Sakellariou and S. H. Anastasiadis, *Macromolecules*, 2017, 50, 4699–4706.
- 29 H. Zhang, S. Kulkarni and S. L. Wunder, *J. Electrochem. Soc.*, 2006, **153**, A239–A248.
- 30 J. Zhang, X. Zang, H. Wen, T. Dong, J. Chai, Y. Li, B. Chen, J. Zhao, S. Dong, J. Ma, L. Yue, Z. Liu, X. Guo, G. Cui and L. Chen, J. Mater. Chem. A, 2017, 5, 4940–4948.
- 31 J. Hu, W. Wang, H. Peng, M. Guo, Y. Feng, Z. Xue, Y. Ye and X. Xie, *Macromolecules*, 2017, **50**, 1970–1980.
- 32 Q. Zheng, L. Ma, R. Khurana, L. A. Archer and G. W. Coates, *Chem. Sci.*, 2016, 7, 6832–6838.
- 33 J.-A. Choi, Y. Kang, H. Shim, D. W. Kim, H.-K. Song and D.-W. Kim, *J. Power Sources*, 2009, **189**, 809–813.
- 34 K. M. Kim, B. Z. Poliquit, Y.-G. Lee, J. Won, J. M. Ko and W. I. Cho, *Electrochim. Acta*, 2014, **120**, 159–166.
- 35 H. Wu, Y. Cao, H. Su and C. Wang, Angew. Chem., Int. Ed., 2018, 57, 1361–1365.
- 36 Q. Pan, D. Barbash, D. M. Smith, H. Qi, S. E. Gleeson and C. Y. Li, Adv. Energy Mater., 2017, 7, 1701231.
- 37 R. L. Hand and R. F. Nelson, J. Am. Chem. Soc., 1974, 96, 850-860.
- 38 Y. Shi, D. J. Noelle, M. Wang, A. V. Le, H. Yoon, M. Zhang, Y. S. Meng and Y. Qiao, ACS Appl. Mater. Interfaces, 2016, 8, 30956–30963.
- 39 Z. Song, Y. Qian, T. Zhang, M. Otani and H. Zhou, Adv. Sci., 2015, 2, 1500124.
- 40 Y. Liang, Y. Jing, S. Gheytani, K.-Y. Lee, P. Liu, A. Facchetti and Y. Yao, *Nat. Mater.*, 2017, **16**, 841.
- 41 Y. Liang and Y. Yao, Joule, 2018, 2, 1690-1706.
- 42 G. A. Horrocks, A. Parija, L. R. De Jesus, L. Wangoh, S. Sallis, Y. Luo, J. L. Andrews, J. Jude, C. Jaye, D. A. Fischer, D. Prendergast, L. F. J. Piper and S. Banerjee, *Chem. Mater.*, 2017, 29, 10386–10397.
- 43 F. Croce, S. Sacchetti and B. Scrosati, *J. Power Sources*, 2006, **162**, 685–689.
- 44 S. Liu, H. Wang, N. Imanishi, T. Zhang, A. Hirano, Y. Takeda, O. Yamamoto and J. Yang, *J. Power Sources*, 2011, **196**, 7681–7686.
- 45 C. N. Walker, C. Versek, M. Touminen and G. N. Tew, *ACS Macro Lett.*, 2012, 1, 737–741.
- 46 K. M. Diederichsen, H. G. Buss and B. D. McCloskey, *Macromolecules*, 2017, **50**, 3831–3840.
- 47 D. Lin, P. Y. Yuen, Y. Liu, W. Liu, N. Liu, R. H. Dauskardt and Y. Cui, *Adv. Mater.*, 2018, **30**, 1802661.
- 48 J. Evans, C. A. Vincent and P. G. Bruce, *Polymer*, 1987, 28, 2324–2328.
- 49 J. Trevey, Y. S. Jung and S.-H. Lee, ECS Trans., 2009, 16, 181–187.
- 50 Y. Tian, T. Shi, W. D. Richards, J. Li, J. C. Kim, S.-H. Bo and G. Ceder, *Energy Environ. Sci.*, 2017, **10**, 1150–1166.
- 51 W. Zhou, H. Gao and J. B. Goodenough, *Adv. Energy Mater.*, 2016, **6**, 1501802.